Project Report
PSM-3

Detecting Gait Asymmetry with Wearable Accelerometers

J.R. Williamson
A. Dumas
A.R. Hess
K. Fischl
T. Patel
B.A. Telfer
M.J. Buller

18 March 2015

Lincoln Laboratory
MASSACHUSETTS INSTITUTE OF TECHNOLOGY
LEXINGTON, MASSACHUSETTS

Prepared for the U.S. Army Research Institute of Environmental Medicine (USARIEM)
under Air Force Contract FA8721-05-C-0002.

This report is based on studies performed at Lincoln Laboratory, a federally funded research and development center operated by Massachusetts Institute of Technology. This work is sponsored by the U.S. Army Research Institute of Environmental Medicine (USARIEM), under Air Force Contract FA8721-05-C-0002.

The 66th Air Base Group Public Affairs Office has reviewed this report, and it is releasable to the National Technical Information Service, where it will be available to the general public, including foreign nationals.

This technical report has been reviewed and is approved for publication.

FOR THE COMMANDER

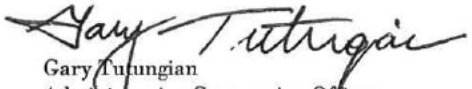

Gary Tutungian
Administrative Contracting Officer
Enterprise Acquisition Division

Massachusetts Institute of Technology
Lincoln Laboratory

Detecting Gait Asymmetry with Wearable Accelerometers

J.R. Williamson
A. Dumas
A.R. Hess
T. Patel
B.A. Telfer
Group 48

K. Fischl
Formerly Group 48

M.J. Buller
U.S. Army Research Institute of Environmental Medicine
Natick, Massachusetts

Project Report PSM-3

18 March 2015

Lexington Massachusetts

This page intentionally left blank.

ABSTRACT

Gait asymmetry can be a useful indicator of a variety of medical and pathological conditions, including musculoskeletal injury (MSI), neurological damage associated with stroke or head trauma, and a variety of age-related disorders. Body-worn accelerometers provide the ability for real-time monitoring and detection of changes in gait asymmetry, thereby providing continuous real-time information about medical conditions and enabling timely interventions. We propose practical and robust algorithms for detecting gait asymmetry using features extracted from accelerometers attached to each foot. By registering simultaneous acceleration differences between the two feet, these asymmetry features provide robustness to a variety of confounding factors, such as changes in walking speed and load carriage. Because the algorithms require only summary statistics obtained from each frame (i.e., contiguous block) of accelerometer data, they can potentially be implemented in real-time physiological status monitoring systems, which may operate under severe limitations in power, computation, and communication bandwidth.

We evaluate the algorithms on a data collection consisting of 24 subjects with multiple levels of induced gait asymmetries in both indoor and outdoor natural walking conditions. Changes in magnitude and pattern asymmetry features are sensitive to the sign and magnitude of gait asymmetry and provide the ability to detect and track asymmetries during continuous monitoring. By creating individualized background models from short data collections of normal walking, the algorithms are able to reliably detect asymmetrical walking induced by small ankle weights during short duration walking trials. Moreover, the background models and the test data are derived from both indoor and outdoor walking trials, where the outdoor walking contained uphill and downhill grades. The best performing features did not require detection of individual strides, using instead sufficient statistics collected independently from each foot over 20 s data frames. Consideration is given to how these statistical features enable real-time asymmetry detection and characterization on body-worn systems.

This page intentionally left blank.

TABLE OF CONTENTS

This page intentionally left blank.

LIST OF FIGURES

This page intentionally left blank.

1. INTRODUCTION

Healthy human gait requires the complex interplay of muscle control, balance, and cognitive function. Asymmetrical gait is an indicator of pathology [1] and has been studied for a variety of musculoskeletal and neurological conditions, including stroke, Parkinson's disease, osteoarthritis, prosthetics, and joint replacement [2–10]. The initial application area motivating this work is the detection of early onset of musculoskeletal injuries caused by overuse. Common overuse injuries include stress fractures, tendinitis, bursitis, fasciitis, and medial tibial stress syndrome (shin splints) [11]. In particular, the military is faced with a "physical training MSI [musculoskeletal injury] epidemic" [12]. MSIs are the leading cause of military medical care visits, disability discharges, and resulting in more medical evacuations than any other cause, including combat injuries [12]. Approximately 40% of MSIs affect the lower extremity [11]. Inexpensive, automated, wearable sensor monitoring could provide early indicators of overuse injuries.

Commercially available wearable accelerometers have the potential to characterize gait asymmetry beyond a laboratory setting. Our interest is practical monitoring of gait characteristics during natural walking, unencumbered by limited video field of view and allowing natural stride period variations not possible on a treadmill. A large body of work assesses gait under laboratory or clinical conditions (ex. [3, 5, 6, 13]) and makes use of stationary equipment such as treadmills, force plates, or multi-camera video systems with fiducial markers. In contrast, using readily available sensors, we aim for a practical system of characterizing abnormal gait by comparing high-resolution accelerometer data from both limbs. Challenges include nonuniform walking surfaces, walking speed, and variations in accelerometer positioning. Inter-stride comparisons of swing and stance timing values between limbs to assess asynchrony tend to be rigid and somewhat impractical outside of a laboratory setting since all sensors must be precisely synchronized.

Several types of features have been investigated by others to assess gait asymmetry: stride-timing (swing- or stance-times) [3, 5, 8, 9], acceleration magnitudes [2, 14], and acceleration time-varying patterns as well as autocorrelation peaks [2, 10, 14, 15]. These features have been primarily assessed in the context of clinical or laboratory measurements compared against normative values. While many studies assume gait symmetry (identical spatiotemporal parameters between limbs) for normative values, this is not necessarily the case, even for healthy individuals [1]. Thus, establishing a healthy baseline and obtaining individualized gait characteristics is useful in evaluating changes over time. Individualized gait asymmetry detection is also important due to intersubject variability. This report has two principal contributions: (1) a novel method for utilizing time-varying autocorrelation pattern features from an accelerometer, and (2) an algorithm for detecting changes in an individual's gait asymmetry, compared to a baseline, in the presence of variations in walking surfaces and speeds.

This page intentionally left blank.

2. METHODS

2.1 DATA COLLECTION

In a study approved by the MIT Committee on the Use of Humans as Experimental Subjects, a total of 24 volunteers between the ages of 18 and 65 wore accelerometers (Actigraph GTX3+) while walking with asymmetrical ankle weights to induce asymmetrical gait. The tri-axial accelerometers measure up to ±6 G, and sample up to 100 Hz. Accelerometers were securely attached to both feet with Velcro straps through the shoelaces to register foot accelerations while reducing turbulence during foot strikes. An example of the actigraph and its placement is shown in Figure 1.

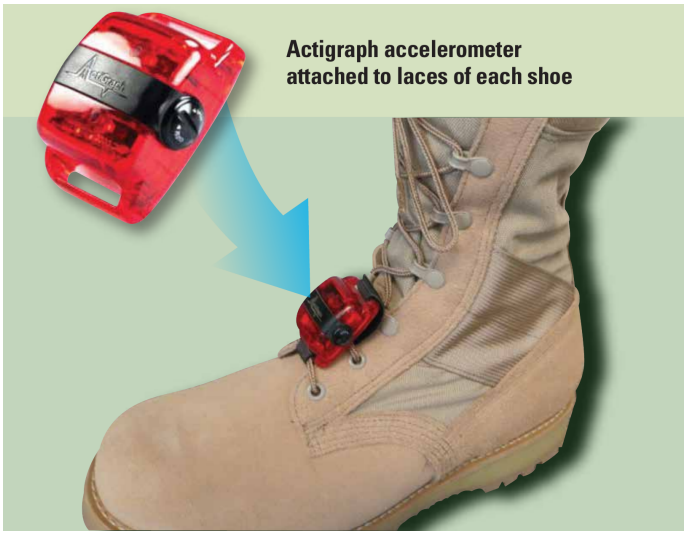

Figure 1. Example placement of Actigraph on shoelaces.

Participants walked in multiple ∼7 minute trials while either wearing no ankle weight or a weight of 1/3, 1/2, 1, or 2 lbs on both ankles (separately). The maximum weight of 2 lbs is less than half of the 5.5 lb weight used by others [16] to induce gait asymmetry. In each session, the order of weights and weighted ankle was randomized; however, the sessions always started and ended with unweighted trials. Trials were conducted both indoors in carpeted hallways and outdoors on a looped 0.4 km gravel path that includes uneven terrain and an 8 meter elevation change. Typically, the indoor and outdoor trials were completed on separate days.

2.2 GAIT ASYMMETRY FEATURES

Our approach has been to maintain approximate (within 1–2 seconds) synchronization from sensor initialization via software. We use sensors that have low clock drift (approximately 30 ppm) and look at acceleration dynamics contained in fixed duration time frames to capture a series of strides. Summary data could be reported wirelessly with low bandwidth requirements to a central processing hub capable of performing further comparative calculations fusing information from

both feet. In this report, we used a desktop computer and offline processing as a surrogate for an embedded hub sensor as proof of concept of feature selection and processing.

We consider features that meet the following implementation constraints: (a) precise knowledge of sensor orientation is not available, (b) precise synchronization between accelerations from the two feet is avoided, and (c) precise walking speed or terrain conditions are not known a priori. To meet constraint (a), features are computed from the instantaneous acceleration magnitudes at the left and right foot. To meet constraint (b), independent summary statistical features are obtained from each foot over fixed time frames, and information fusion across the feet is only done using these summary statistics. Constraint (c) is addressed by evaluating the algorithm on indoor and outdoor walking on different grades at naturally occurring cadences. In addition, all considered features involve simple, easily implementable computations at the foot sensor nodes. The features considered can be separated into two types: (1) *frame-based* features, which are statistical measures over the frame time interval that do not rely on detections of individual stride events, and (2) *stride-based* features, which are statistical measures over the frame that rely on detections of fiducial stride events, such as heel strike and toe-off. An overview of the processing steps required is shown in Figure 2.

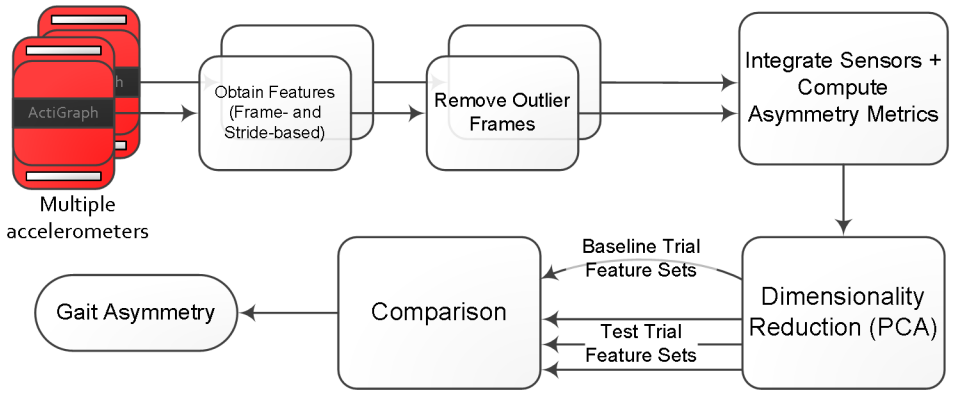

Figure 2. Overview of processing steps required for gait asymmetry detection using accelerometry. PCA = principal component analysis.

2.2.1 Frame-based Features

Previous versions of these features have been used to predict subjective reports of ambulatory distress in soldiers conducting a series of 5 km outdoor marches in different loading conditions [17]. The frame-based features can be separated into *magnitude* features, which assess properties of total acceleration magnitude, and *pattern* features, which assess properties of acceleration dynamics, irrespective of total magnitude. In the current study, summary features are computed within 20 s data frames with 10 second overlap. These features summarize the average properties from several strides and reduce communication requiring only intermittent reporting of summary statistics from

sensor nodes to the hub. The magnitude features consist of symmetry indices [18],

$$\mathrm{SI}(x, y) = \frac{x - y}{0.5(x + y)}, \tag{1}$$

which are computed from three statistical measures of the left (x) and right (y) foot acceleration magnitude. These measures, which have been found to be useful for movement characterization in other applications [19], are the standard deviation (σ), mean (μ), and coefficient of variation (σ/μ). An alternative feature that combines (σ) and (μ) into a single value is root mean square (RMS) [20, 21].

Whereas the magnitude features register differences in total acceleration magnitude between the two feet, the pattern features register differences in the temporal stride dynamics after the magnitude differences have been factored out. The stride dynamics are captured using autocorrelations of the acceleration magnitude signals. Autocorrelation peaks have been used previously to characterize gait from a single accelerometer [14]. We consider a different approach using the autocorrelation function out to the first peak (capturing a single stride), and computing the differences between the autocorrelations of the two feet. Pattern asymmetry features are then obtained by applying principal component analysis (PCA) [22] of the high-dimensional autocorrelation features.

As a preprocessing step for the pattern features, in order to reduce the effect of the gravity component on each of the three acceleration axes, adjusted acceleration magnitudes (b_t^L and b_t^R), are computed by subtracting the long-term median acceleration value from each axis. In practice, the median subtraction was done on data collected from each subject within a single day. The temporal dynamics are then captured by computing autocorrelations for the right and left foot over delay samples, k, ranging from 0 to 2 s:

$$d_i^L(k) = \frac{1}{(n_i - k)} \sum_{t, t+k \in f_i} c_t^L c_{t+k}^L, \tag{2}$$

$$d_i^R(k) = \frac{1}{(n_i - k)} \sum_{t, t+k \in f_i} c_t^R c_{t+k}^R, \tag{3}$$

where $c_t^L = (b_t^L - \mu_{\mathbf{b},i}^L)/\sigma_{\mathbf{b},i}^L$ and $c_t^R = (b_t^R - \mu_{\mathbf{b},i}^R)/\sigma_{\mathbf{b},i}^R$.

To obtain *time-scaled* autocorrelation patterns that span one stride period, the average stride period in each frame, g_i, is first estimated by selecting the peak in the summed autocorrelation patterns, $\mathrm{argmax}_i(\mathbf{d_i^L} + \mathbf{d_i^R})$. The range of possible stride durations is constrained to be between 0.5 and 1.5 seconds, a range that easily encompasses all walking strides during this study. To obtain more precise estimates of the stride durations, cubic interpolation of the summed autocorrelation functions is used, sampled at 10 kHz to mitigate the effects of quantization. Lower sampling rates could presumably be used for interpolation, should the performance requirements demand it with limited hub hardware. The g_i values are employed to compute time-scaled autocorrelation patterns that span one stride period:

$$e_i^L(k) = d_i^L(k/g_i), \tag{4}$$

$$e_i^R(k) = d_i^R(k/g_i). \tag{5}$$

Single-frame gait asymmetry vectors are obtained from these patterns in a manner similar to the symmetry index:

$$\mathbf{x}_i = \frac{\mathbf{e}_i^L - \mathbf{e}_i^R}{\sqrt{||\mathbf{e}_i^L||^2 + ||\mathbf{e}_i^R||^2}}. \tag{6}$$

The top half of Table 1 lists four combinations of the frame-based magnitude and pattern features that are evaluated in this study.

2.2.2 Stride-based Features

Common features used in the context of quantifying asymmetrical gait relate to particular subphases of the gait. These prominently include the stance time, in which the foot is in contact with the ground, and the swing time, in which it is in motion [23–26]. The ratio of stance time to total stride duration, which we refer to as duty factor, has also been used [3, 5, 27]. The analogous ratio of swing time to stride duration is referred to as swing factor [24]. Some features used in the past relate to the gait subphases: the *heel-strike*, when the heel impacts the ground, and *toe-off*, when the toe leaves the ground [24]. Gait studies often use force sensors in a clinical setting. Force features used in the past include the peaks of the impulse of the heel-strike [28] and toe-off force and the integral of the force over the course of the stride [13, 23].

Extracting similar features requires identification of steps and step subphases from the acceleration magnitude signal. The orientation of the accelerometers on the foot while stationary is not perfectly level and also will vary over the course of a stride with respect to gravity. This makes the isolation of the gravity vector and determination of the true orientation difficult. The step identifier operates on the magnitude of the acceleration rather than one particular component so that it is independent of orientation.

Stride duration is relatively easily identifiable from the periodicity of the acceleration magnitude. However, identification of subphases of the gait requires more detailed examination. In the development of the step identifier, accelerometer data was collected simultaneously with force sensor data for comparison. The step identifier is based on time-domain analysis of the acceleration signal for each foot separately. The flow chart in Figure 3 summarizes this algorithm.

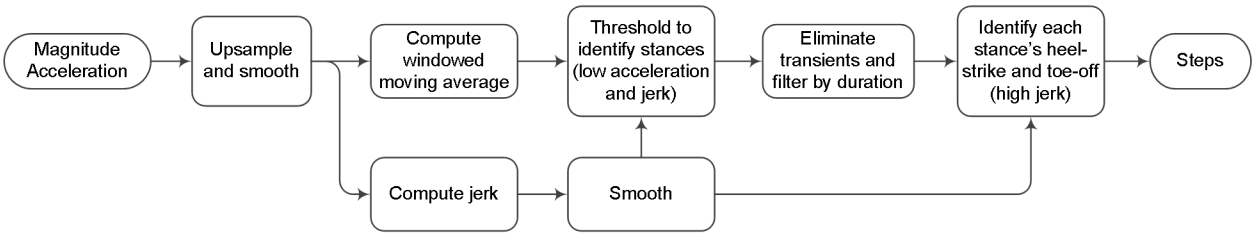

Figure 3. Flow chart showing processing steps required to extract stride-based features by identifying individual steps in the acceleration magnitude time series. Jerk is defined as the first derivative of the acceleration magnitude.

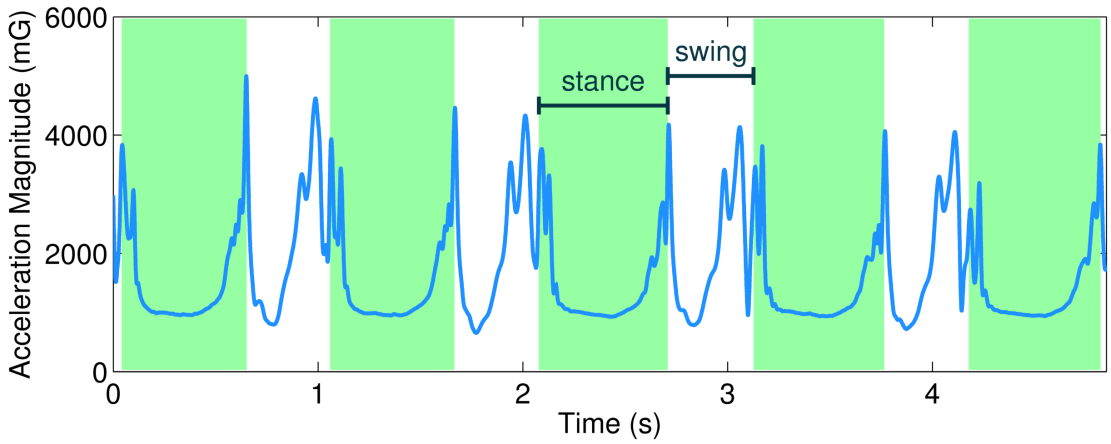

Figure 4. Example of automatic segmentation of step, stance (green background), and swing (white background) times based on acceleration magnitude (blue) for several steps.

Stances are characterized by acceleration that is stable at 1 g (acceleration due to gravity) when the foot is stationary on the ground. To identify these instances, the acceleration magnitude and its first derivative (known as jerk) are upsampled to 1 kHz (from the original 100 Hz sampling rate), smoothed using boxcar averaging, and then low-pass filtered to reduce noise. Potential stance times are identified as periods when the acceleration magnitude is approximately 1 g, and the jerk magnitude is under a specified threshold. Low jerk with acceleration near 1 g indicates that the foot is motionless on the ground, with gravity as the predominant component of the measured acceleration. These candidate stance values are then thresholded using a range of reasonable step durations to remove outliers.

Heel-strike and toe-off of the step are then identified. These are periods when the foot is rapidly decelerating as it impacts the ground and rapidly accelerating as it leaves the ground. Consequently, both are characterized by impulses in acceleration magnitude on either side of identified stance times, with high acceleration and high jerk. Heel-strike and toe-off times are determined by extending outward from the identified stance time into areas of the signal with sufficiently high acceleration and jerk. The algorithm finds the peak of the smoothed jerk in these regions, which corresponds to noisy impulses in the original magnitude signal. From this, the stance time is then computed as the difference of toe-off time and heel-strike time. The swing time is the heel-strike time minus the toe-off time of the previous step. Figure 4 shows an example of the step, stance, and swing times identified from an acceleration magnitude signal across several steps. The acceleration magnitude is shown in blue. The stance time is shown shaded in green, with the swing time in white.

Once the steps and stride phases have been identified, several other candidate features are extracted. For each step, the mean, variance, and RMS value of the acceleration and jerk are extracted. These statistics are also extracted for the stance and swing subphases. Other extracted features are the peak acceleration for the heel-strike and toe-off for each step, and the integrated acceleration over the course of the step. These features are conceptually similar to features from

force measurements that have been used [13,23]. Multiple features are derived from the acceleration and jerk measures by integrating them over (a) total stride duration, (b) stance time, and (c) swing time. Features that rely on time synchronization between the two feet are not considered, due to the focus in this study on potential real-time applications without frequent communication or synchronization.

Summary stride-based statistical features are obtained from the raw stepwise features using 20 second time windows with 10 seconds of overlap. These features fall into two basic categories: those related to the timing of the stride phases and those relating to characteristics of the acceleration magnitude during those phases. Features were evaluated to find those most useful in identifying gait asymmetries induced by the ankle weights, with the most useful stride-based features listed in the bottom half of Table 1. These are the stepwise integrated acceleration magnitude (IA), the mean acceleration magnitude during the stride (MA), the peak stride acceleration (PA), the foot contact time (FCT), the swing time (ST), and the duty factor (DF). Table 1 summarizes all of the major features for each feature category, as well as the best-performing feature combinations. Many other features and feature combinations were also evaluated, but they performed similarly or worse to those in Table 1.

TABLE 1

Summary of Features Used Together and Individually to Distinguish Gait Conditions

Feature Name	Feature Category	Feature Description
RMS	Frame, Mag.	SI of $\sqrt{\sigma^2 + \mu^2}$
Magnitude	Frame, Mag.	SI of $\{\sigma, \mu, \sigma/\mu\}$
Pattern	Frame, Pattern	PCA of $\mathbf{x}$ in eq. (6)
Frame Comb.	Frame, Both	SI of σ, PCA of $\mathbf{x}$ in eq. (6)
IA	Stride, Mag.	SI of Integrated Accel.
MA	Stride, Mag.	SI of Mean Acceleration
PA	Stride, Mag.	SI of Peak Acceleration
FCT	Stride, Timing	SI of Foot Contact Time
ST	Stride, Timing	SI of Swing Time
DF	Stride, Timing	SI of Duty Factor
Stride Comb.	Stride, Both	PCA of stride features

RMS = root mean square; Mag. = magnitude; SI = symmetry index; Comb. = combination; PCA = principal component analysis; IA = integrated acceleration; MA = mean acceleration; PA = peak acceleration; FCT = foot contact time; ST = swing time; DF = duty factor.

2.3 COMPENSATING FOR STRIDE VARIABILITY

One of the confounding factors affecting the gait asymmetry features is changes in stride rate. We found that a slower stride rate (and hence longer stride periods) tends to reduce the magnitude of gait asymmetry features given the same weight condition. With sufficient amounts of data, we could learn statistical models of how to adjust the features, conditioned on the stride period. For now, we have opted simply to weight the features in frame i by a function of average stride period in that frame, g_i^2, in order to amplify feature values obtained during long stride periods. We have found that this adjustment improves asymmetry detection performance for all of the features and feature combinations listed in Table 1.

2.4 OUTLIER FRAME REMOVAL

In constructing statistical models of normal walking, from which to characterize or detect asymmetrical deviations, it is important to first select which data frames predominantly consist of walking. There are many ways that this can be done. We have selected walking frames using the time-scaled autocorrelation patterns in an iterative outlier removal procedure. The procedure, applied independently to each data trial, is as follows. First, the time-scaled autocorrelation patterns are concatenated,

$$\mathbf{e}_i = [\mathbf{e}_i^L, \mathbf{e}_i^R]. \tag{7}$$

Then, using the index j to indicate valid frames, we start with all frames labeled as valid: $\{j\} \equiv \{i\}$. In each iteration of the procedure, the distribution of $\mathbf{e}_j$ vectors is modeled using an independent Normal distribution, $N(\mu_{\mathbf{e}}, \sigma_{\mathbf{e}})$, computed from the valid frames $\{j\}$. If the maximum Mahalanobis distance between the valid frames and the Normal distribution is < 2, then the iterative procedure stops. Otherwise, the frame with the maximum distance is relabeled as invalid, and the iterative procedure continues.

2.5 DIMENSIONALITY REDUCTION

Multiple highly correlated features can be transformed into a more useful representation using principal component analysis (PCA), in order to obtain a smaller set of decorrelated features containing the greatest amount of variance. PCA is used for the frame-based pattern features and for combining the stride-based features. Before applying PCA, we first normalize feature elements $x_j(k)$, where j is the frame index and k is the vector element index, into standardized units,

$$y_j(k) = (x_j(k) - \mu_{\mathbf{x}(k)})/\sigma_{\mathbf{x}(k)}. \tag{8}$$

For gait asymmetry *characterization* (Section 3.2), $\mu_{\mathbf{x}(k)}$ and $\sigma_{\mathbf{x}(k)}$ are computed from all of a subject's trials. For gait asymmetry *detection* (Section 3.3), they are computed from all of the unweighted trials that comprise a subject's background model. Principal component features are then computed, and the PCA conversion parameters are applied to the features from any held-out trials.

This page intentionally left blank.

3. RESULTS

3.1 DATA COLLECTION SUMMARY

From the 24 participants, a total of 456 trials were acquired over the aforementioned weight conditions. The histogram in Figure 5(a) shows the distribution of trial durations for all conditions indoors and outdoors. The median indoors trial duration was 6.6 ± 1.2 minutes and the median outdoor trial duration was 6.5 ± 2.5 minutes. The box plot in Figure 5(b) shows the trial durations across weight conditions, where there were no significant differences between durations of any of the conditions.

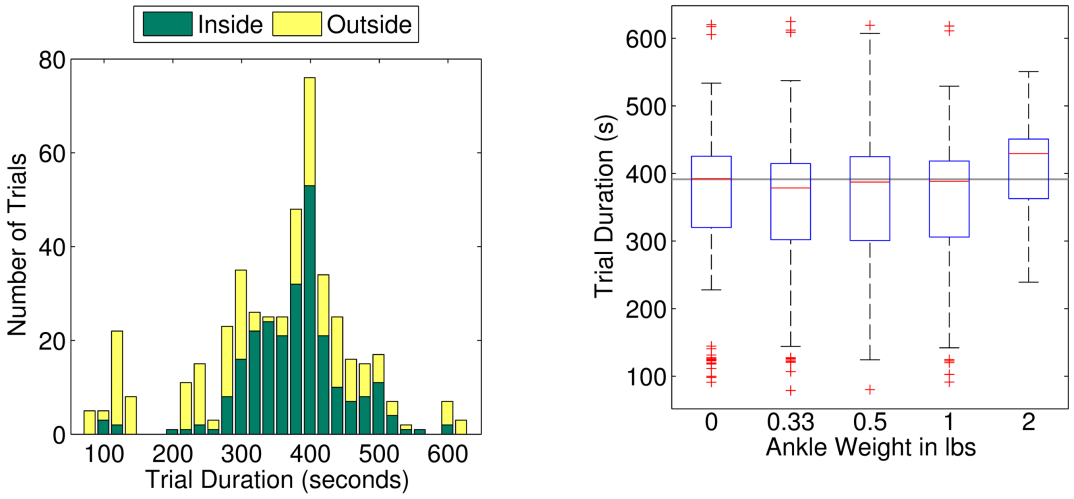

(a) (b)

Figure 5. A histogram of data collection trial durations in all conditions (N=456 trials) is shown above in (a). Trial durations are also shown in (b) by weight configuration. The median trial duration, shown as a gray horizontal line in (b), was 391 ± 117 seconds (or 6.5 ± 1.9 minutes).

The number of acquired trials per individual was mostly uniform, with a few exceptions, as can be seen in Figure 6, which shows the number of unweighted trials both indoors and outdoors per subject, as well as in Figure 7, which shows the number of weighted trials per subject. The median number of trials for each subject is five with no weight (three inside, two outside) and four with each of the weighted conditions. Certain subjects acquired more unweighted trials when their data collection was split across multiple days, since each data collect started and ended with an unweighed indoor trial regardless of which conditions were collected. Subjects who volunteered to collect 2 lb data have additional unweighted trials as well for the same reason. Most subjects have four trials per weight condition since each weight was used indoors and outdoors and on each foot.

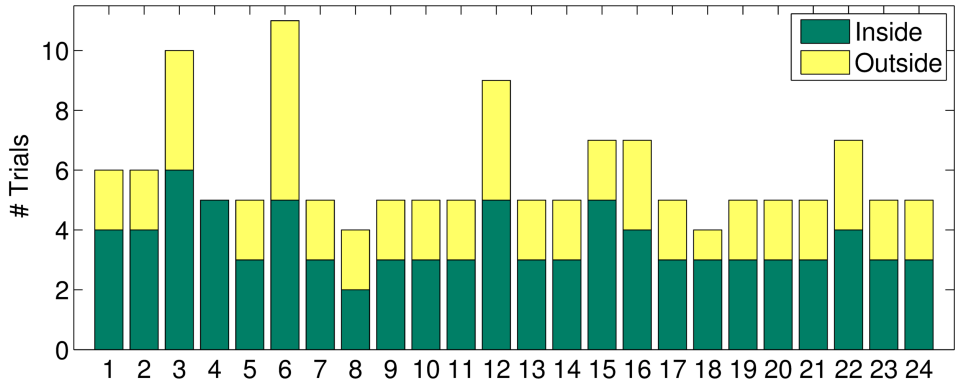

Figure 6. Number of normal (unweighted) trials collected by subject ID.

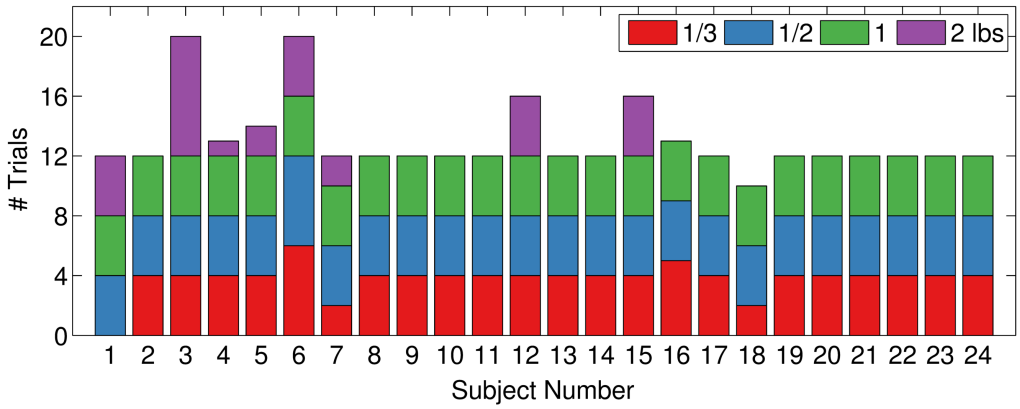

Figure 7. Number of weighted trials acquired per subject, where most of the conditions have two trials per weight (one from each foot) collected indoors and outdoors.

3.2 CHARACTERIZATION OF GAIT ASYMMETRY

To illustrate gait asymmetry features as a function of stride period, we consider subject 6, from whom the largest number of trials were obtained: 31 trials from four sessions over a four-month period. Figure 8 plots, for all 31 trials, frame-based stride periods estimated by the autocorrelation method described in Section 2.2. Stride period varies by about 10% and varies more on the outdoor trials due to the presence of uphill and downhill grades. Figure 9 shows that frame-based magnitude feature 1, which is the symmetry index of the standard deviation of acceleration magnitude, tracks well with ankle weights despite stride-period variations. Features from unweighted gait trials are similar, and close to zero, across multiple trials (and days) and across terrain conditions (indoors versus outdoors). Features from weighted trials indicate the sign of asymmetry, and tend toward larger deviations with larger induced asymmetries. Outdoor trials in general produce greater variations in magnitude feature 1 than indoor trials do. This is likely due to the presence of uphill and downhill grades, and possibly also due to unevenness of the gravel walking path.

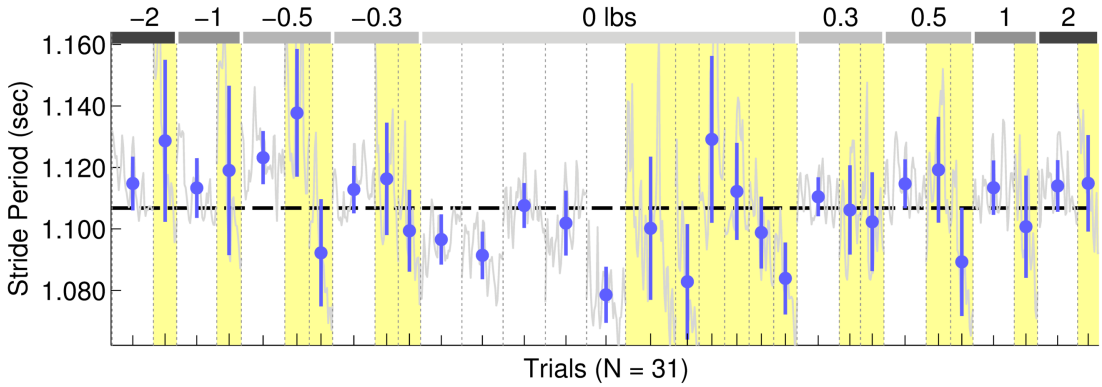

Figure 8. Frame-based stride periods, g_j, are plotted as a function of frame index j and asymmetry (weight) value for all 31 trials of subject 6. The values above the figure denote ankle weights, with negative values corresponding to weight placement on the right ankle. Valid frames only (i.e., non outliers) are plotted in this figure (and in subsequent figures as well). Trials are delimited by dashed vertical lines. Outdoor trials are denoted by yellow shading.

The purpose of the pattern features is to register asymmetries in the temporal acceleration dynamics in a way that is relatively invariant to changes in cadence and in acceleration magnitude. Figure 10 displays in an image format the feature vectors from equation (6) following cross-frame normalization. Figure 10 illustrates clear differences due to both weight conditions and terrain conditions. Figure 11 plots jointly the first magnitude feature and the first pattern principal component for subject 6, for varying weight conditions. Unweighted data tends to center around the origin, while weighted data is spread in the feature space to reflect differentiation between left- and right-ankle weight application.

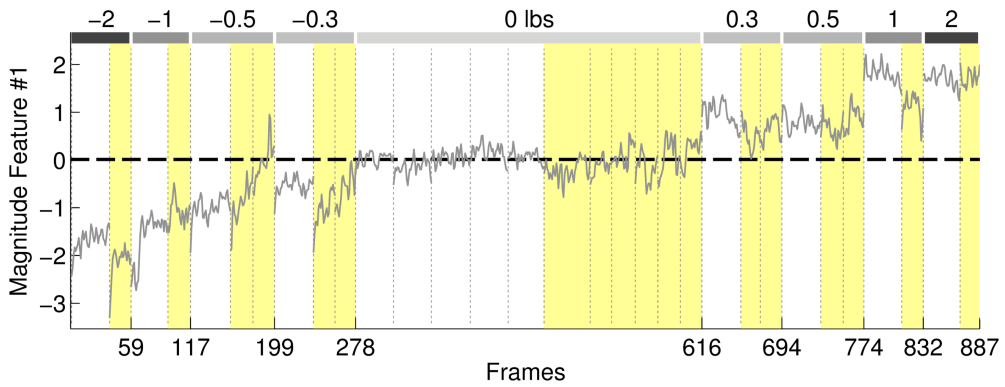

Figure 9. Magnitude feature 1 is the symmetry index of the standard deviation of acceleration magnitude, computed over 20 s frames. The normalized version of this feature is plotted (in units of standard deviation) for subject 6, with trials sorted by asymmetry value: $W_L - W_R$, where W_L is the weight on the left ankle, and W_R is the weight on the right ankle. Trials are separated by dotted vertical lines. Outdoor trials are shaded yellow.

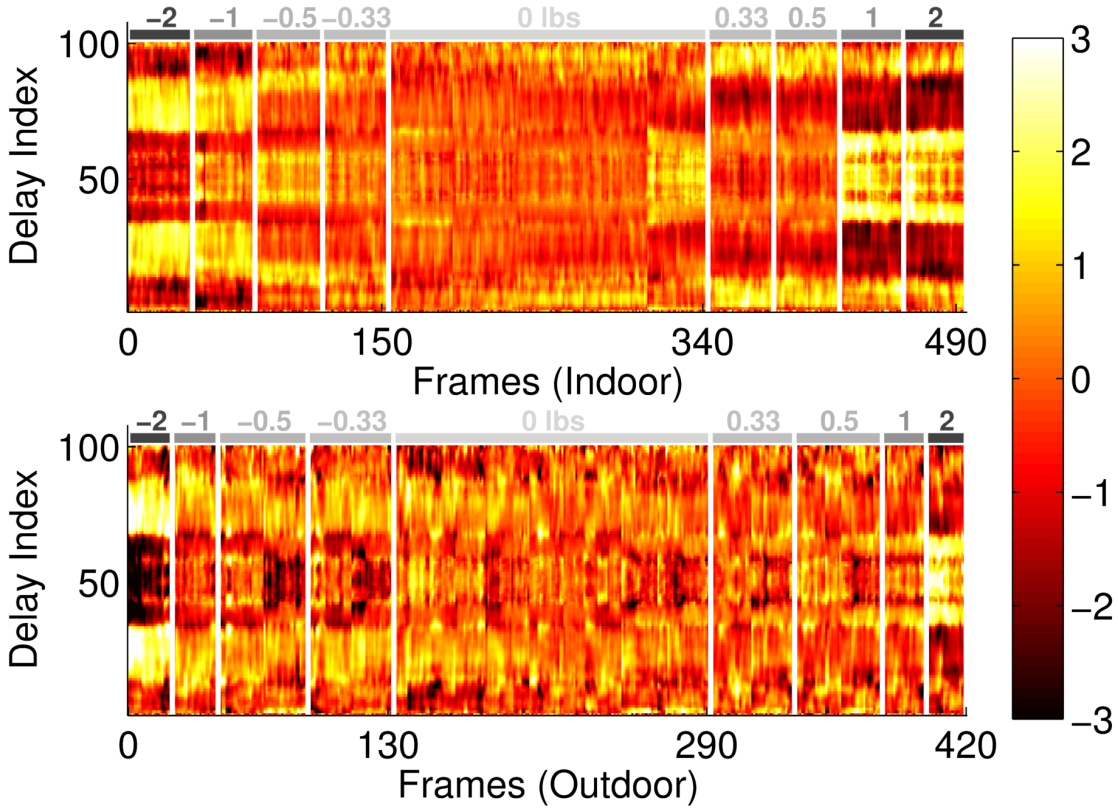

Figure 10. Frame-based pattern asymmetry feature vectors, $\mathbf{x_i}$, are plotted after cross-frame normalization. Values indicate pattern features in units of standard deviation as a function of stride delay index.

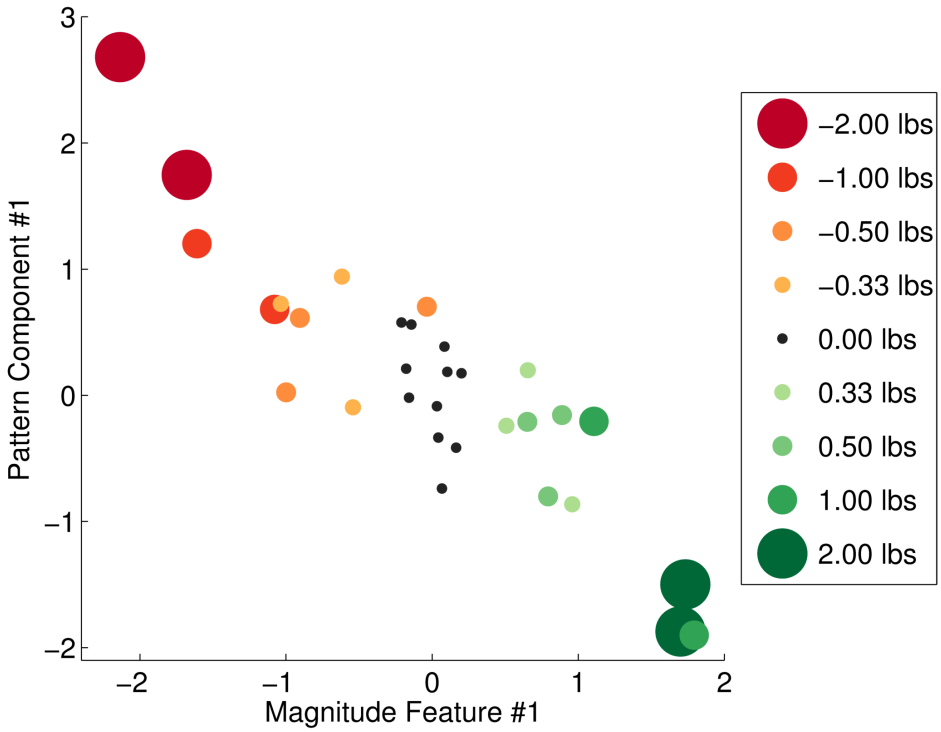

Figure 11. Plot of mean values from first magnitude and pattern components over each trial from 31 trials for subject 6. On the x-axis is the first magnitude feature, and on the y-axis is the first frame-based pattern principal component. Black circles indicate unweighted trials, shades of red indicates trials with weight on right ankle, and green indicates trials with weight on left ankle. Marker size distinguishes varying asymmetry values (larger indicates larger absolute value of asymmetry condition).

3.3 DETECTION PERFORMANCE

Asymmetry detection performance is quantified through receiver operating characteristics (ROCs) and the areas under these curves (AUCs). For each subject, a background model is generated from unweighted trials. Given the background model, the average feature likelihoods from each test trial are computed, and ROCs are generated by varying the likelihood threshold. We restricted the number of trials comprising the background model to three, allowing at least one held-out baseline trial for all subjects. For each subject, all possible combinations of three baseline trials were tested against the held-out baseline trials and averaged.

Figure 12 shows ROCs from subject 6 for one of the most effective feature combinations: the first magnitude feature and the first four pattern asymmetry components. Average AUCs of 1.00 and 0.99 were achieved for ankle weights of 2 and 1 lbs, respectively. AUC histograms across all subjects for different ankle weights are shown in Figure 13, using the same (best-performing) feature combination assessed in Figure 12. The mean AUC values for 1/3, 1/2, 1, and 2 lbs are 0.66, 0.75, 0.92, and 0.98 respectively.

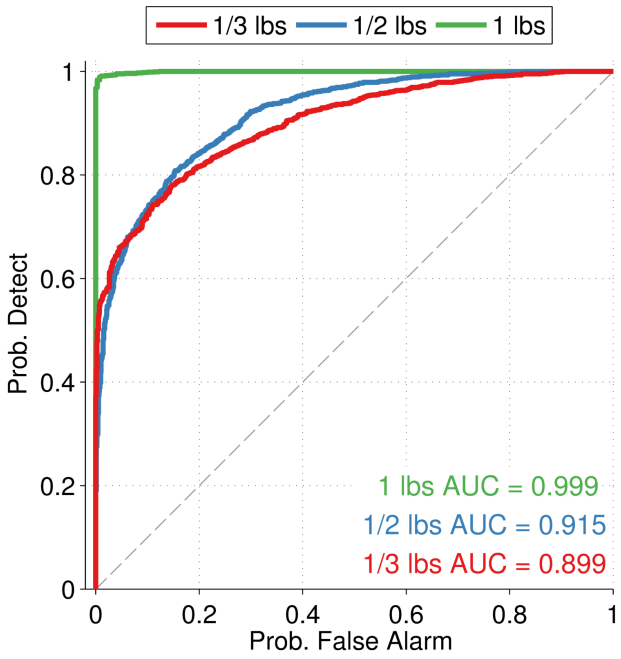

Figure 12. ROCs for subject 6 based on background models obtained from three unweighted trials and computed separately for the four weighted conditions. Features used are the first frame-based magnitude feature and the first four frame-based pattern principal components. Not shown: for 2 lb weight, AUC was 1.0.

The following feature set combinations were also considered, with the mean AUC values for each summarized in Figure 14:

(1) Frame-based: RMS feature

(2) Frame-based: three magnitude features

(3) Frame-based: ten pattern principal components

(4) Frame-based: first magnitude feature & first four pattern principal components *(best performing)*

(5) Stride-based: integrated acceleration feature

(6) Stride-based: duty factor feature

(7) Stride-based: six principal components from multiple features

These results show that several combinations of features produce similar results, with the best average AUC values obtained using the combined frame-based features (feature set 4, in Figure 14).

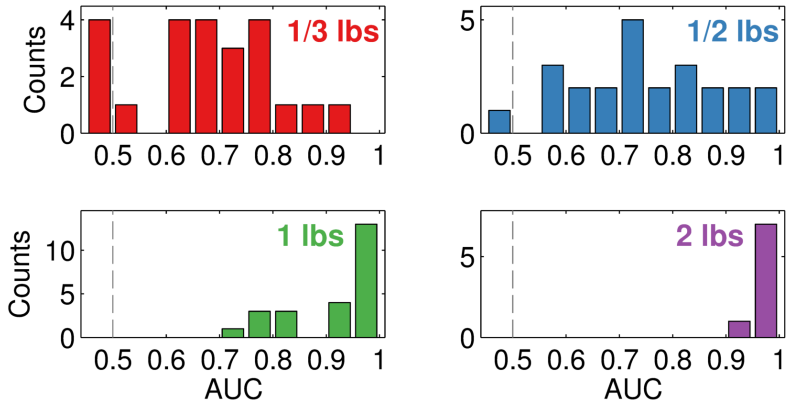

Figure 13. AUC histograms for all subjects in the four weighted conditions, using the first frame-based magnitude feature and the first four frame-based pattern principal components.

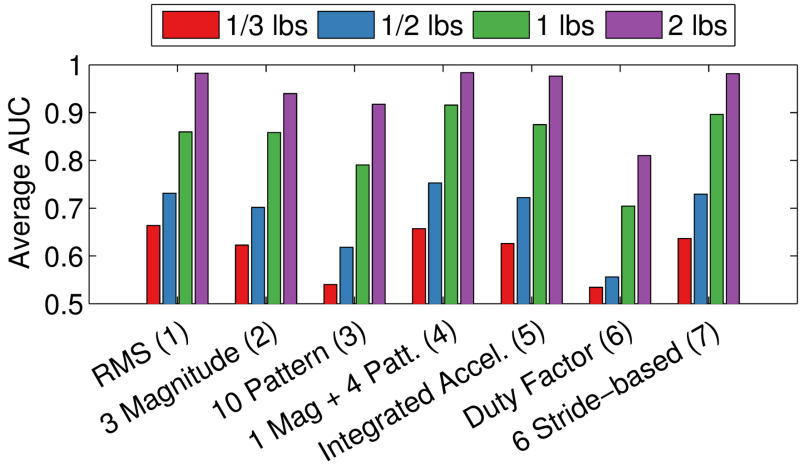

Figure 14. Average AUC values for the four weight conditions, from seven different feature combinations.

However, statistically significant differences ($p < .05$) are found only between two groups of features: those that include acceleration magnitudes (feature sets 1, 2, 4, 5, and 7) and those that do not (sets 3 and 6). Statistical significance was tested using the Wilcoxon-Mann-Whitney rank sum test [29] applied to AUC values from all of the weight conditions and all 24 subjects.

Lastly, we consider the effect of the number of baseline trials used to compute the background model. For a subset of 6 subjects who collected at least 7 baseline trials, Figure 15 contains the AUC values for the frame-based combined features, as a function of the number of baseline trials used to form the background model. Performance improves as the number of baseline trials increases, which bodes well for the continuous monitoring that we envision. Also note that, for larger asymmetry values (1 and 2 lbs), performance is above 0.9 AUC even with just two background trials to train against.

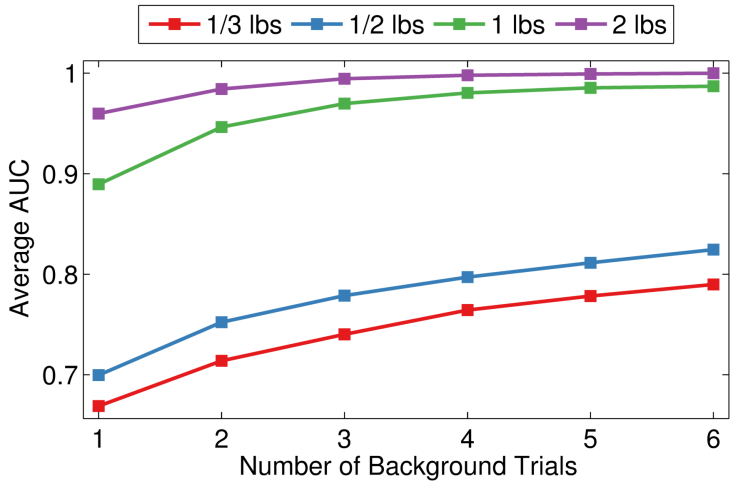

Figure 15. Average AUC values for four weight conditions are plotted, obtained from subjects 3, 6, 12, 16, and 22 using the combined frame-based features. AUC values are plotted as a function of the number of normal trials used to create the background model. The average duration of walking data used to create the background models varies from 6.5 minutes (1 trial) up to 39 minutes (6 trials).

3.4 CASE STUDY: GAIT ASYMMETRY DURING INJURY RECOVERY

A natural question is: How do the artificially induced gait asymmetries compare to an actual overuse injury? This question is provisionally addressed by analyzing data from subject 1, who developed iliotibial (IT) band syndrome, a common overuse injury [30], several weeks after the ankle weight data was collected. In order to track recovery, one trial of indoor walking was recorded over six days (Friday, then Monday through Friday of the following week). Figure 16 plots the first magnitude feature and the pre-PCA pattern features over the six days. The subject reported discomfort and exhibited limping in the first two collections (Friday and Monday). The gait asymmetry features are consistent with these subjective reports.

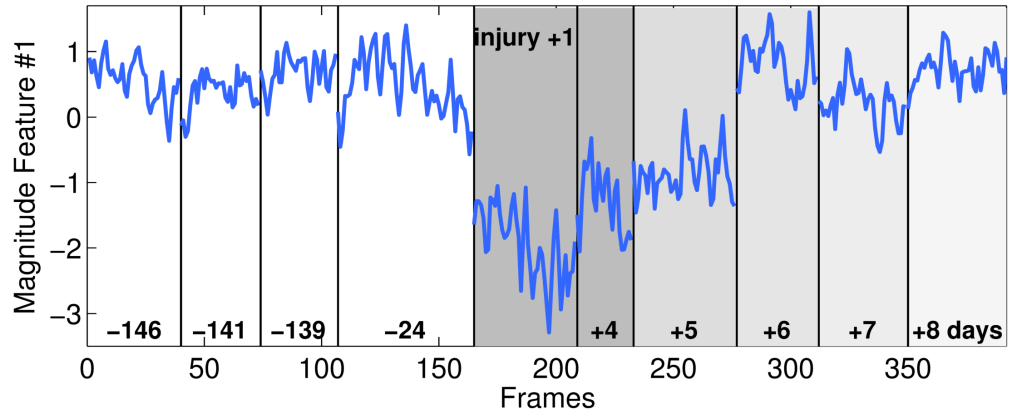

(a) Magnitude feature values before injury and during recovery.

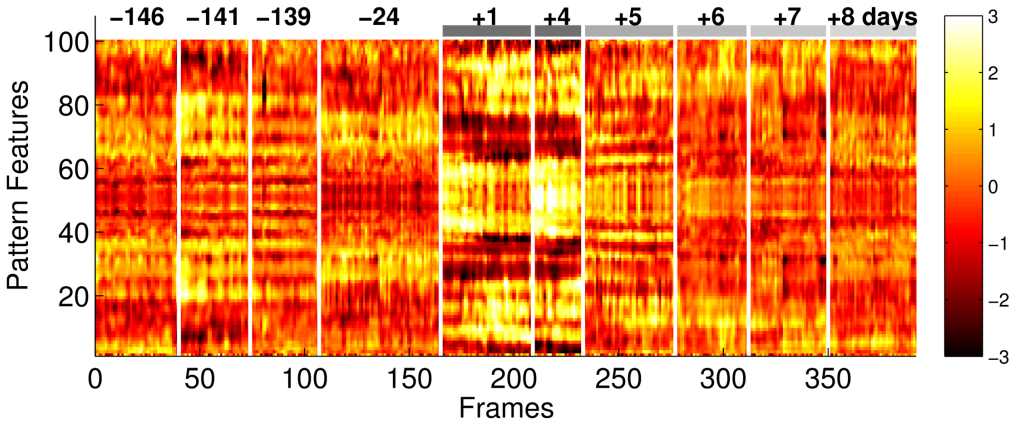

(b) Pattern feature values before injury and during recovery.

Figure 16. Frame-based magnitude feature values for subject 1 are shown in (a), before and after repetitive stress injury. Magnitude and pattern features are plotted in units of standard deviation from mean (following cross-frame normalization, described in Section 2.5).

Prior to the injury, the magnitude feature during unweighted bouts in Figure 16(a) shows relative agreement across days. After the injury, however, the magnitude feature becomes negative, indicating a right-foot asymmetry. During the course of recovery (around 6–7 days following the injury), the magnitude feature returns to its pre-injury baseline. The multidimensional pattern features show a result that is more difficult to interpret visually. However, immediately after the injury (+1 and +4 days), they are clearly different from pre-injury values in both their value and pattern. Notably, the pattern features show the greatest deviation from normalcy on day +4, when the subject reported the greatest level of discomfort and stopped walking halfway through the trial. Overall, this small-scale case study suggests that the feature set presented in this report has potential for detecting actual muskuloskeletal injuries.

4. CONCLUSION

From acceleration magnitudes measured on both feet during walking with artificially induced asymmetries, we have derived a set of features that provide discriminative value in detecting and characterizing the asymmetry. In a test on 24 subjects, several sets of features were found to be most promising with respect to maximizing detection accuracy: (1) frame-based magnitude features or RMS acceleration, (2) frame-based magnitude feature 1 with pattern principal components, (3) stride-based integrated acceleration, and (4) stride-based principal components. By fusing frame-based magnitude and pattern features that do not require detection of individual strides, each class of asymmetries was detected with higher accuracy than with any other feature combination. However, a statistically significant advantage was not found compared to the best four alternative feature combinations.

The performance of the stride-based features is generally comparable to, but slightly worse than, that of the frame-based features. The best single frame-based feature, RMS, slightly outperforms the best single stride-based feature, which is IA. The combined frame-based magnitude and pattern features similarly outperform the six principal components from multiple stride-based features. In addition to improving performance over the stride-based features, the frame-based features do not require the precise segmentation of each individual step, or of intra-step components.

In terms of area under the receiver operation characteristic (ROC) curve, the detection performance using the best feature combination, for the asymmetry levels of 1/3, 1/2, 1, and 2 lbs can be summarized as mean AUC values of 0.66, 0.75, 0.92, and 0.92, respectively. Moreover, this was done using only three trials per subject to create a background model. We also showed, for a subset of subjects, strong improvements of detection performance as more trials were added to the creation of the background model.

Testing on artificially induced asymmetries is convenient for proof of concept, but clearly has limitations in that the relation of these asymmetries to asymmetries caused by injury is not well defined. However, our algorithm was trained only on unweighted trials, and therefore demonstrates the general ability to detect deviations from normal gait. The detection algorithm is based on the average likelihoods in test trials given the background model. Thus, any significant deviation from the background will be detected. As an example of this, the gait asymmetry from one subject's IT band injury was detected. The effect of this injury on magnitude and pattern features was similar to that caused by a 1 lb weight. The algorithm is also the first known to the authors that is individualized rather than based on normative comparisons, and that has been tested outdoors on nonuniform surfaces.

Since the algorithm was originally designed with embedded hardware and near real-time operation in mind, further development and integration must be made with wearable sensor nodes and other hardware to create a system based on the feature selection and processing outlined in this report. For the frame-based features, signal processing requirements at the sensor nodes is very modest (computing first- and second-order statistics within 20 second data frames), with small requirements for communication bandwidth to the central processing hub. The processing

requirements for the central hub include constructing and periodically updating the background statistical model as more data are collected.

Our primary goal is to utilize these features to detect actual injuries, with the quantification of rehabilitation progress as a logical future continuation. The features could also possibly be used as an indicator of other pathologies associated with gait asymmetry [1–10], to assess progress toward performance optimization in locomotion, or to inform the metabolic costs associated with locomotion in each leg [31]. With regard to these goals, the current results raise relevant questions for algorithm maturation, such as: What is the difference in detection performance for different walking surfaces? Is it important to first identify which portions of the data were collected on a smooth walking surface? Can the algorithm be applied to running data? Why is the detection performance better for some subjects than others? We plan to address these questions by more thoroughly evaluating the aforementioned features in larger, follow-on field studies.

REFERENCES

[1] H. Sadeghi, P. Allard, F. Prince, and H. Labelle, "Symmetry and limb dominance in able-bodied gait: a review," *Gait & Posture* 12(1), 34–45 (2000).

[2] C. Mizuike, S. Ohgi, and S. Morita, "Analysis of stroke patient walking dynamics using a tri-axial accelerometer," *Gait & Posture* 30(1), 60–64 (2009).

[3] K.K. Patterson, W.H. Gage, D. Brooks, S.E. Black, and W.E. McIlroy, "Evaluation of gait symmetry after stroke: a comparison of current methods and recommendations for standardization," *Gait & Posture* 31(2), 241–246 (2010).

[4] R. Meijer, M. Plotnik, E.G. Zwaaftink, R.C. van Lummel, E. Ainsworth, J.D. Martina, and J.M. Hausdorff, "Markedly impaired bilateral coordination of gait in post-stroke patients: Is this deficit distinct from asymmetry? a cohort study," *Journal of Neuroengineering and Rehabilitation* 8(1), 23 (2011).

[5] A. Salarian, H. Russmann, F.J. Vingerhoets, C. Dehollaini, Y. Blanc, P.R. Burkhard, and K. Aminian, "Gait assessment in parkinson's disease: toward an ambulatory system for long-term monitoring," *Biomedical Engineering, IEEE Transactions on* 51(8), 1434–1443 (2004).

[6] J.J. Kavanagh and H.B. Menz, "Accelerometry: a technique for quantifying movement patterns during walking," *Gait & Posture* 28(1), 1–15 (2008).

[7] S.J.M. Bamberg, R.J. Carson, G. Stoddard, P.S. Dyer, and J.B. Webster, "The lower extremity ambulation feedback system for analysis of gait asymmetries: preliminary design and validation results," *JPO: Journal of Prosthetics and Orthotics* 22(1), 31–36 (2010).

[8] C.B. Redd and S.J.M. Bamberg, "A wireless sensory feedback device for real-time gait feedback and training," *Mechatronics, IEEE/ASME Transactions on* 17(3), 425–433 (2012).

[9] K. Aminian, K. Rezakhanlou, E. De Andres, C. Fritsch, P.F. Leyvraz, and P. Robert, "Temporal feature estimation during walking using miniature accelerometers: an analysis of gait improvement after hip arthroplasty," *Medical & Biological Engineering & Computing* 37(6), 686–691 (1999).

[10] C. Hodt-Billington, J.L. Helbostad, W. Vervaat, T. Rognsvåg, and R. Moe-Nilssen, "Criteria of gait asymmetry in patients with hip osteoarthritis," *Physiotherapy Theory and Practice* 28(2), 134–141 (2011).

[11] K.G. Hauret, B.H. Jones, S.H. Bullock, M. Canham-Chervak, and S. Canada, "Musculoskeletal injuries: description of an under-recognized injury problem among military personnel," *American Journal of Preventive Medicine* 38(1), S61–S70 (2010).

[12] B.C. Nindl, T.J. Williams, P.A. Deuster, N.L. Butler, and B.H. Jones, "Strategies for optimizing military physical readiness and preventing musculoskeletal injuries in the 21st century," *US Army Medical Department Journal* (4-13), 5–23 (2013).

[13] R.A. Zifchock, I. Davis, J. Higginson, and T. Royer, "The symmetry angle: a novel, robust method of quantifying asymmetry," *Gait & Posture* 27(4), 622–627 (2008).

[14] R. Moe-Nilssen and J.L. Helbostad, "Estimation of gait cycle characteristics by trunk accelerometry," *Journal of biomechanics* 37(1), 121–126 (2004).

[15] A. Tura, M. Raggi, L. Rocchi, A.G. Cutti, and L. Chiari, "Gait symmetry and regularity in transfemoral amputees assessed by trunk accelerations," *J Neuroeng Rehabil* 7(4) (2010).

[16] D. Gouwanda and S. Arosha Senanayake, "Identifying gait asymmetry using gyroscopes– a cross-correlation and normalized symmetry index approach," *Journal of Biomechanics* 44(5), 972–978 (2011).

[17] J.R. Williamson, K. Fischl, A. Dumas, A. Hess, T. Hughes, and M.J. Buller, "Individualized detection of ambulatory distress in the field using wearable sensors," in *Body Sensor Networks (BSN), 2013 IEEE International Conference on* (2013), pp. 1–6.

[18] R. Robinson, W. Herzog, and B. Nigg, "Use of force platform variables to quantify the effects of chiropractic manipulation on gait symmetry." *Journal of manipulative and physiological therapeutics* 10(4), 172–176 (1987).

[19] J.R. Williamson, D.W. Bliss, D.W. Browne, P. Indic, E. Bloch-Salisbury, and D. Paydarfar, "Individualized apnea prediction in preterm infants using cardio-respiratory and movement signals," in *Body Sensor Networks (BSN), 2013 IEEE International Conference on* (2013), pp. 1–6.

[20] M. Yang, H. Zheng, H. Wang, S. McClean, J. Hall, and N. Harris, "Assessing accelerometer based gait features to support gait analysis for people with complex regional pain syndrome," in *Proceedings of the 3rd International Conference on PErvasive Technologies Related to Assistive Environments*, ACM (2010), p. 48.

[21] R. Yamaguchi, S. Hirata, T. Doi, T. Asai, J. Inoue, D. Makiura, H. Ando, M. Kurosaka, and Y. Miura, "The usefulness of a new gait symmetry parameter derived from lissajous figures of tri-axial acceleration signals of the trunk," *Journal of physical therapy science* 24(5), 405–408 (2012).

[22] C.M. Bishop, *Neural networks for pattern recognition*, Oxford university press (1995).

[23] L. Nolan, A. Wit, K. Dudziñski, A. Lees, M. Lake, and M. Wychowañski, "Adjustments in gait symmetry with walking speed in trans-femoral and trans-tibial amputees," *Gait & posture* 17(2), 142–151 (2003).

[24] M.G. Benedetti, V. Agostini, M. Knaflitz, V. Gasparroni, M. Boschi, and R. Piperno, "Self-reported gait unsteadiness in mildly impaired neurological patients: an objective assessment through statistical gait analysis," *Journal of neuroengineering and rehabilitation* 9(1), 1–7 (2012).

[25] A. Shrinivasan, M. Brandt-Pearce, A. Barth, and J. Lach, "Analysis of gait in patients with normal pressure hydrocephalus," in *Proceedings of the First ACM Workshop on Mobile Systems, Applications, and Services for Healthcare*, ACM (2011), p. 3.

[26] J.W. Noble and S.D. Prentice, "Adaptation to unilateral change in lower limb mechanical properties during human walking," *Experimental brain research* 169(4), 482–495 (2006).

[27] H. Skinner and R. Barrack, "Ankle weighting effect on gait in able-bodied adults." *Archives of physical medicine and rehabilitation* 71(2), 112–115 (1990).

[28] H.H. Manap, N.M. Tahir, and A.I.M. Yassin, "Anomalous gait detection based on support vector machine," in *Computer Applications and Industrial Electronics (ICCAIE), 2011 IEEE International Conference on*, IEEE (2011), pp. 623–626.

[29] W.J. Conover and R.L. Iman, "Rank transformations as a bridge between parametric and nonparametric statistics," *The American Statistician* 35(3), 124–129 (1981).

[30] F.A. Barber and A.N. Sutker, "Iliotibial band syndrome," *Sports Medicine* 14(2), 144–148 (1992).

[31] R.W. Hoyt and P.G. Weyand, "Advances in ambulatory monitoring: using foot contact time to estimate the metabolic cost of locomotion," *Emerging Technologies for Nutrition Research: Potential for Assessing Military Performance Capability*, pp. 315–343 (1996).

This page intentionally left blank.

REPORT DOCUMENTATION PAGE

Form Approved
OMB No. 0704-0188

1. REPORT DATE *(DD-MM-YYYY)*	**2. REPORT TYPE**	**3. DATES COVERED** *(From - To)*
18 March 2015	Project Report	

4. TITLE AND SUBTITLE

Detecting Gait Asymmetry Changes with Wearable Accelerometers

5a. CONTRACT NUMBER
FA8721-05-C-0002

5b. GRANT NUMBER

5c. PROGRAM ELEMENT NUMBER

6. AUTHOR(S)
J.R. Williamson, A. Dumas, A.R. Hess, T. Patel, B.A. Telfer, and K. Fischl, MIT Lincoln Laboratory, and M.J. Butler, USARIEM

5d. PROJECT NUMBER
2170

5e. TASK NUMBER
0

5f. WORK UNIT NUMBER

7. PERFORMING ORGANIZATION NAME(S) AND ADDRESS(ES)

MIT Lincoln Laboratory
244 Wood Street
Lexington, MA 02420-9108

8. PERFORMING ORGANIZATION REPORT NUMBER

PSM-3

9. SPONSORING / MONITORING AGENCY NAME(S) AND ADDRESS(ES)
U.S. Army Research Institute of Environmental Medicine
15 Kansas Street
Natick, MA 01760

10. SPONSOR/MONITOR'S ACRONYM(S)
USARIEM

11. SPONSOR/MONITOR'S REPORT NUMBER(S)

12. DISTRIBUTION / AVAILABILITY STATEMENT
Approved for public release; distribution is unlimited.

13. SUPPLEMENTARY NOTES

14. ABSTRACT

Gait asymmetry can be a useful indicator of a variety of medical and pathological conditions, including musculoskeletal injury (MSI), neurological damage associated with stroke or head trauma, and a variety of age-related disorders. Body-worn accelerometers provide the ability for real-time monitoring and detection of changes in gait asymmetry, thereby providing continuous real-time information about medical conditions and enabling timely interventions. We propose practical and robust algorithms for detecting gait asymmetry using features extracted from accelerometers attached to each foot. By registering simultaneous acceleration differences between the two feet, these asymmetry features provide robustness to a variety of confounding factors, such as changes in walking speed and load carriage. Because the algorithms require only summary statistics obtained from each frame (i.e., contiguous block) of accelerometer data, they can potentially be implemented in real-time physiological status monitoring systems, which may operate under severe limitations in power, computation, and communication bandwidth.

We evaluate the algorithms on a data collection consisting of 24 subjects with multiple levels of induced gait asymmetries in both indoor and outdoor natural walking conditions. Changes in magnitude and pattern asymmetry features are sensitive to the sign and magnitude of gait asymmetry and provide the ability to detect and track asymmetries during continuous monitoring. By creating individualized background models from short data collections of normal walking, the algorithms are able to reliably detect asymmetrical walking induced by small ankle weights during short duration walking trials. Moreover, the background models and the test data are derived from both indoor and outdoor walking trials, where the outdoor walking contained uphill and downhill grades. The best performing features did not require detection of individual strides, using instead sufficient statistics collected independently from each foot over 20 s data frames. Consideration is given to how these statistical features enable real-time asymmetry detection and characterization on body-worn systems.

15. SUBJECT TERMS

16. SECURITY CLASSIFICATION OF:			**17. LIMITATION OF ABSTRACT**	**18. NUMBER OF PAGES**	**19a. NAME OF RESPONSIBLE PERSON**
a. REPORT	**b. ABSTRACT**	**c. THIS PAGE**			**19b. TELEPHONE NUMBER** *(include area code)*
Unclassified	Unclassified	Unclassified	Same as report	36	

This page intentionally left blank.